International Journal of New Technology and Research (IJNTR)
ISSN:2454-4116, Volume- 2, Issue-5, May 2016 Pages 16-25

Investigation of Elemental Radioactive Concentrations and Radon Gas in Soil Samples Collected Around Abou Zabal Fertilizer Phosphate Factory

S.Fares, W.M.Moslem, A.K.Hassan, A.A.Eltawil, F.Abdelhamied

***Abstract*- Determine levels of some natural radioactivity in soil samples were collected around Abou Zabal fertilizer phosphate factory in Egypt. Activity concentration of the soil sample of ^{226}Ra, ^{232}Th and ^{40}K was determined by using a high resolution γ -ray HPGe spectrometry and CR-39 detector. According to the results this analysis, ^{238}U was found concentration mean (241.06 ± 23.17 Bqkg^{-1}), ^{226}Ra was found in concentrations mean of (283.87 ± 26.53 Bq kg^{-1}), ^{232}Th in mean concentrations of (16.15 ± 1.45 Bq kg^{-1}) and ^{40}K in mean concentrations of (146.36 ± 6.9 Bq kg^{-1}) for the analyzed soil, respectively. Radon (^{222}Rn) mean concentration in the samples was estimated using solid state nuclear track detectors (CR – 39). The Radon gas mean doses from inhalation gas were found (337.06.37 µSv/y). The radioactivity levels determined and the γ-absorbed dose rates in soil sample above the ground were calculated. Elemental concentrations were determined for ^{226}Ra (range from 7.8 ppm to 46.26 ppm), ^{232}Th (range from 1.98 ppm to 9.14 ppm), ^{238}U (from 5.63 ppm to 33.28 ppm), and ^{40}K (from 0.07 % to 0.69 %). The measured Th/U ratio exhibits values was mean 0.17 , whereas the U/Ra ratio was mean 0.81 and Th/K ratio values was mean 0.8 there are unequilibrium between ^{232}Th and ^{40}K but there are equilibrium between ^{238}U and ^{226}Ra . Correlation Coefficient between Mass exhalation and Activity concentration of ^{238}U equal (1.0). Correlation Coefficient between Surface exhalation and Activity concentration of ^{238}U equal (0.962777) this was very good correlation. Correlation Coefficient between Activity concentration of ^{226}Ra e and Activity concentration of ^{238}U equal (0.962777) the good correlation.**

***Key words*: (CR – 39), XRD, Soil, pollution, natural radioactivity contents and.**

I. INTRODUCTION

Uranium and its decay products are found in phosphate rocks of sedimentary origin. Now, these phosphates are largely used for the production of phosphoric acid and fertilizers. Their radio activities result in health problems from radiation at the level of the industrial processes for the preparation of fertilizers as well as for the fertilizers themselves at the origin of radioactivity dispersion in the geo- and biospheres. On the other hand, leaching of the minerals and of the wastes is another source of dissemination and possible transfer to waters and finally to the living beings. During the past decades, around phosphate fertilizer factory Abou Zabal activities in the Egypt widely expanded causing an escalation in the application of inorganic fertilizers, pesticides and other phosphate fertilizer chemicals to increase crop production and to enhance soil properties. Inorganic, specially phosphate (P), fertilizers contain hazardous elements including, heavy metals, e.g. Cd, Cr, and Pb, and radioactive elements, e.g. U, Th and their daughters, which are considered to be toxic to human and animal health [1]. Due to the long-continued application of inorganic fertilizers, these heavy metals and radionuclides will be added and could be accumulated in soil, i.e. their concentrations, as contaminants their concentrations in fertilizers, annual application rate of fertilizers, in soil can increase over time [2]. The contaminants accumulation in soil due to long-continued phosphate fertilizer activities will depend on, physical and chemical properties of soil and geochemical properties of the contaminant.

Naturally occurring phosphate rocks (PRs) differ widely in their mineralogy and chemistry. The chemical reactivity or solubility of phosphate rocks is a measure of the PR's ability to release P for plant uptake. Reactivity is defined by Rajan et al. (1996) as 'the combination of PR properties that determines the rate of dissolution of the PR in a given soil under given field conditions.' The reactivity of sedimentary phosphate rocks is relatively high compared to those of igneous and metamorphic origin. The fundamental difference lies in the crystal chemistry of apatite, specifically the degree of isomorphous substitution of phosphate by carbonate. It has been shown that the solubility of carbonate substituted phosphate rocks is higher than the solubility of pure fluorapatite with little or no carbonate-substitution. Increasing carbonate substitution in the phosphate rock increases the ease of breakdown of the structure of the apatite thereby releasing P to the soil solution under acidic conditions. The chemical and mineralogical features are key factors in determining the reactivity and subsequent agronomic effectiveness of a given phosphate rock. The crystal-chemical composition of apatite's can be analyzed by several methods, including X-ray diffraction (XRD)

S.Fares, 1-Department of Radiation Physics, National Center for Radiation Research and Technology NCRRT, Atomic Energy Authority, Cairo, Egy.

2-Department of Physics , Faculty of Science, Baha University, Saudi Arabia 00966532811239

W.M.Moslem, Department of Physics , Faculty of Science, Port Said University Egypt (wmmoslem@hotmail.com).

A.K.Hassan, Department of Physics , Faculty of Science, Baha University, Saudi Arabia

A.A.Eltwil, Armed forces Main chemical laboratory Egypt

F.Abdelhamied, Department of Physics , Faculty of Science, Port Said University Egypt.

analyses. The XRD patterns of apatite provide an array of peaks that are typical for the crystal-composition of the apatite. Slight shifts in the peak positions and intensities indicate shifts in the crystal chemistry of the mineral. Changes in composition of the mineral can be determined by specific crystallographic parameters, for example the unit-cells of the crystallographic a-axis. Early work by [3,4]established the relationship between changes in the apatite crystal chemistry, specifically substitution in the apatite, and the so-called unit-cell a-values.

II. EXPERIMENT AND METHODLOGY

A. The study areas

The fertilizer production facility, located in El Abou Zabal, produces single superphosphate and triple superphosphate at a combined capacity of 1,600 MT/day. The facility resides on a 350,000 sq m plot area and is divided into two zones. The first comprises fertilizer production and auxiliary facilities stretching over a total expanse of 207,000 sq m. The second is reserved for future production of sulphuric acid. Ideally located 500 m away from the Nile River banks, the facility is assured of a secure water supply source that is vital for its industrial/domestic uses and cost-effective operations. Abou Zabal Fertilizer & Chemical Company 1947 - Operations began. Owned by Polyserve Fertilizers and Chemicals Group, Abou Zabal Fertilizer and Chemical Factory were established in 1974 to manufacture all kinds of phosphate fertilizers and chemicals. In 2002 the factory was privatized and acquired by Polyserve Fertilizers & Chemicals Company. Plant No. 1 Coordinates 30° 16' 34" N, 31° 22' 45" E, Plant No. 2 Coordinates 30° 16' 42" N, 31° 22' 46" E.

.

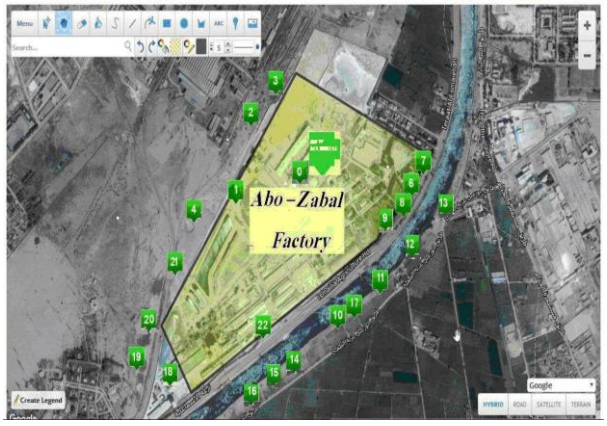

Fig (1). Site collecting soil samples around Abou- Zabal fertilizer factory.

B. Sampling and Samples Preparation

Soil sampling and sample preparation

Soil samples were collected from 23 locations in the area of the study, as shown in figure (1) samples were collected using the core method with a depth of about 20 cm. Two composite samples were collected from each location, one from cultivated land (inside the circle) and the other one from uncultivated land (outside the circle). Samples were dried in open air dry place, mechanically crushed, and sieved through a 2 mm mesh sieve. For gamma-ray spectrometry, aliquot of each sample was transferred to a plastic container of 300 cc capacity and sealed for about four weeks to reach secular equilibrium between ^{226}Ra and ^{228}Ra, and their progenies [5]. Fertilizer soil samples were collected from around Abou Zabal factory. These samples were oven-dried at 110 °C for 24 h to remove humidity. Then, the fertilizer soil samples were grinded and sieved through a 2 mm nylon mesh to ensure homogeneity. Each 20 g of these fertilizer samples was transferred to separate plastic cans (5.5 cm diameter × 10 cm height) and was then sealed. Each sample was equipped with a CR-39 plastic track detector (1.5 cm × 1.5 cm), produced by the Track Analysis Systems Ltd., Napier House, Meadow Grove, Bristol, UK. The detector was fixed at the top inside of the cans lid prior to closing.

C. Gamma Ray Spectrometer:

1- HPGe detector

The soil samples from area of the study were analyzed using a high-resolution; low-back ground gamma-ray spectrometry system based on a coaxial high purity germanium detector (HPGe). The diameter of the crystal is 62.10 mm and was operated under a high voltage, bias of (+) 3000 V (DC). The unwanted ambient radioactivity from room background sources was reduced by surrounding the detector with a cylindrical lead shield of about 10 cm thickness. The gamma-ray spectra which were analyzed were created through converting the event energy into a pulse height spectrum. The signal processing was done by connecting the detector to a preamplifier and a standard spectroscopy shaping amplifier. The resultant spectral was analyzed using Canberra Genie software “Genie-2000” [6].

2- CR-39 detector

The concentration and exhalation rate of radon can be made using CR-39 detectors because of their capability to register tracks at different levels of registration sensitivity. The detector (CR-39) calibration should be performed where the integrating radon’s concentration is known [7]. The CR-39 detectors used in this work were supplied by Pershore Mouldings, Ltd., UK, in the form of large sheets which were cut into 2 cm2 cm squares. The sample was placed in a glass cylinder of radius 3.5 cm and 10 cm length. Dosimeters were prepared by putting two (CR-39) detectors in the bottom of the chamber cover. The cylindrical container was sealed; the samples were stored for at least 30 days. The determination of the concentrations of alpha particles emitted from radon gas in soil samples were performed by using the nuclear track detector (CR-39) of thickness (250 μm) and area of about (1×1cm2). The radon gas concentration in soil samples was obtained by using the sealed-cup technique. After the irradiation time (45 day), the (CR-39) track detectors were etched in (6.25 N), (NaOH) at temperature of (60 Co) for (6 h), and the tracks density were recorded using an optical microscope with magnification (400x).The density of the tracks (ρ) in the samples were calculated according to the following relation [8].

3- X-ray Diffraction (XRD)

A sample of the prepared powder materials are put in an appropriate aluminum holder. XRD patterns of the slab samples of the prepared were then measured. Here, XRD scanning was carried out by a fully computerized X-ray

Diffractometer, (Shimadzu type XD-6000). Block diagram of the Diffractometer is. Filtered copper radiation, λ=1.542A, was used in this investigation. The X-ray tube was operating at 40 kV and 30 mA anode current throughout the measurements. The pattern was recorded at a scanning rate of 40/min. The above operation conditions were maintained during all the relevant measurements. Hence, it is a plot of the intensity against the angle 2θ, where θ is the reflection angle of X-ray given in Bragg's equation: 2d Sin Θ = nλ.

D. RESULTS AND DISCUSSION

1- Activity concentration samples analysis

The activity concentrations were calculated after measurement and subtraction of the background. The activities were determined from measuring their respective decay daughters [9].The activity concentrations were calculated from the intensity of each line taking into account the mass of the sample, the branching ratios of the γ -decay, the time of counting and the efficiencies of the detector [10,11] . The activity concentrations of the investigated samples were calculated from equation (1):

$$A = (CSP)_{net} / I \times E_{ff} \times M \quad (1)$$

where A is the activity concentration in Bq/kg, $(cps)_{net}$ is the (count per second), I is the intensity of the γ-line in a radionuclide, E_{ff} is the measured efficiency for each γ-line observed and M is the mass of the sample in kilograms. The correction for the contribution of ^{232}Th via its daughter nuclide ^{228}Ac (1459.2 keV peak) to the 1460.8 keV peak of ^{40}K was made according to [12,13]:

$$\text{The error in } ^{40}\text{K activity (\%)} = 9.3(A_{Th}/A_K) \quad (2)$$

A_{Th} and A_K are the activity concentration of ^{232}Th and ^{40}K respectively in Bq/kg

2- Conversion from activity concentration to Elemental concentrations ppm:

Calculate the activity of any sample at any selected energy, and then the weight of ^{238}U isotope can be calculated in order to estimate their concentrations from the well-known formula.

$$C = \frac{W_i}{W_s} \text{ ppm} \quad (3)$$

Where: Wi is the weight of the calculated isotope, Ws is the weight of the sample. In order to determine the background due to the naturally occurring radionuclides in the environment around the detector, any empty container of the same (300 cm3) volume was counted. Isotopes concentration usually expressed in terms of part per million (i.e.) microgram per gram and in terms of specific activity Bq/kg,

1 lg/g = 258.46 Bq/kg for ^{40}K (4)

1 μg/g = 3.654 x 107 Bq/kg for ^{226}Ra (5)

1 μg/g = 12.365 Bq/kg for ^{238}U) (6)

Was calculated from the following formula.

3- Radon and radium concentration

Calculated radon and radium concentration of the soil samples from the following formula:

$$\text{Specific activity} = 6.02x10^{23} x \frac{\lambda}{A} \quad (7)$$

Where λ is the decay constant of isotope, A is the atomic number of isotope. The effective radium content and mass in addition to surface exhalation rate of radon were also measured for the same sample using CR-39 detectors because of their high sensitivity to register alpha particles emitted from the daughters that hit the CR-39 foil, leaving latent damage tracks. After the exposure of a certain time period, the CR-39 was taken out and the latent tracks in it were made visible microscopically under definite etching conditions, the number of tracks was counted. The number of tracks per unit area is proportional to the accumulated concentration of air borne radon. The effective radium concentration of the soil samples can be calculated from the formula [14].

$$C_{Ra}(Bqlkg) = (\frac{\rho}{K T_e}).(\frac{h.A}{M}) \quad (8)$$

where M is the mass of samples (0.025 kg), A is the area of the cross-section of cylinder in m^2 ($A=2\pi r^2$, r is the radius of the cylinder equal to r = 0.011 m), h is the distance between the detector and the top of the solid sample in m that equal to (0.095 m), ρ is the number of tracks per cm^2, K is the radon diffusion constant that equals to 1.23 9 10-3 track/cm^2 h/Bq/m^3 at the radius of cylinder (maintained above) and Te denotes, by definition to the effective exposure time given by [14]:

$$T_e = \left[T - \lambda_{Rn}^{-1}(1-\exp(\lambda_{Rn}T))\right] \quad (9)$$

Where T is the exposure time (61 day), λ_{Rn} is the decay constant of radon. The mass, surface exhalation rate of the sample for the radon is given by [14]:

$$C_{Rn}(Bq/kgday^{-1}) = C_{Ra}\frac{\lambda_{Ra}}{\lambda_{Rn}}.\frac{1}{T_e}$$
$$C_{Rn}(Bq/m^2.day^{-1}) = CRa\frac{\lambda_{Ra}}{\lambda_{Rn}}.\frac{M}{T_e.A} \quad (10)$$

Where: λ_{Ra} is the decay constant of radium.

Dose rate calculation the references [15,17] gave the dose conversion factors for converting the activity concentration of ^{238}U, ^{232}Th and ^{40}K into dose (nGy h^{-1} per Bq kg^{-1}) as 0.427, 0.662 and 0.041 respectively. Using these factors, the total absorbed gamma dose rate in air at 1 m above the ground level is calculated modified from the references. Results and discussion of the average activity concentration in Bq/kg of ^{238}U, ^{226}Ra and ^{40}K and in ppm units of ^{238}U and ^{40}K in the limestone soil of selected samples area of the study are listed in Table (2) using gamma ray spectroscopy. The samples S1-S6 and S21 had high uranium and radium concentration and the radium activity of all selected sample was less than 370 Bq/kg which is within an acceptable safe limit [13]. Samples S0-S6 had high potassium concentration in comparison with other samples. The effective radium concentration and mass, surface exhalation values for radon of limestone rocks in

different locations are listed in Table (3) Samples No. S0 to S6 had high concentration of effective radium and radon using CR-39 detectors.

The high radium and uranium are attributed to secular equilibrium among members and they follow the uranium (4n + 2) series. Due to this fact, many radon anomalies have been interpreted in the past uranium ones. The ^{214}Bi isotope emitted high intensity clear peaks from ^{238}U which means that the measurement of ^{214}Bi peaks is commonly applied to evaluating ^{238}U concentration [19]. It is evident from Table (3) that the effective radium concentration for sample S7-S20, S22 and S23 limestone soil is quite low (in general) varying between 1.78 and 5.78 Bq/kg. It is seen from the same Table (3) that Abou Zabal location with samples (S0 to S6) exhibits the highest exhalation rate (81.82 10^{-6} Bq/kg day^{-1} and 62.88 10^{-6} Bq/m2 day^{-1}), while the samples from (S7 ton S23) in area of the study exhibits the lowest exhalation rate (57.82 10^{-6} Bq/kg day^{-1} and 20.06 10^{-6} Bq/m2 day^{-1}). It is seen too from the same Table (3) that Abou Zabal location with samples (S0 to S6) mass exhibits the highest exhalation rate (122.94 10^{-8} Bq/kg day^{-1} and 94.48 10^{-8} Bq/m2 day^{-1}), while the samples from (S7 ton S23) in area of the study exhibits the lowest exhalation rate (86.44 10^{-8} Bq/kg day^{-1} and 30.14 10^{-8} Bq/m2 day^{-1}). Going back to Table (2) reveals, that the activity of potassium is in the mean range from (146.36 ± 6.9 Bq/kg with 0.57 %) and the activity of uranium is in the mean range from (241.06 ± 23.17 to 33.218.30 ppm) , while the activity of radium is in the range (283.87 ± 26.53 to 25.64 Bq/kg).

The values of all studied radionuclides are considered to be typical level for the region as compared with different sample of soil to the measurement done for in eastern Desert and Nile valley in Egypt [21]. They are also comparable with soil samples from Surda copper deposited in Singhbhum Shear zone in India [22] especially for potassium and uranium concentrations and for rock samples of eastern India [23]. The values of the radium activity, radon exhalation rate from the soil samples are found to be corresponding with the values of uranium concentrations measured by HPGe detector for the same samples. From Fig. (7 a, b, c), it is evident that there is a strong linear relation (R2 =1.0) between the activity concentration of radium, radon exhalation and uranium. Figure (6) shows the activity concentration of uranium, potassium and radium in the collected samples.

4- Correlation studies:

In order to find the extent the existence of these radioactive nuclides together at a particular place, correlation studies were performed between the combinations of radionuclides like ^{226}Ra ,^{238}U, ^{232}Th, and ^{40}K. A search was carried out to detect the presence of a statistically significant correlation between the measured radionuclides in the present rock samples. In fact, the knowledge of the secular equilibrium conditions is necessary in order to make correct assumptions for the dose assessments [17]. In this context and considering all samples, regarding Fig.(7) which shows linear regression of the activity concentrations of ^{238}U versus ^{226}Ra for all samples. As can be seen in Fig.(7), concentrations of ^{238}U and ^{226}Ra showed a statistically significant .

(1) Simple Regression - Mass exhalation Activity concentration of ^{238}U

Activity Correlation Coefficient = 1.0. The output shows the results of fitting a linear model to describe the relationship between Mass exhalation and Activity concentration of ^{238}U. The equation of the fitted model is

$$\text{Mass exhalation} *10^{-8} = 0.000159918 + 0.239184* C_U \quad (11)$$

Since the P-value in the ANOVA table is less than 0.05, there is a statistically significant relationship between Mass exhalation and Activity concentration of ^{238}U at the 95.0% confidence level. The R-Squared statistic indicates that the model as fitted explains 100.0% of the variability in Mass exhalation. The correlation coefficient equals 1.0, indicating a relatively strong relationship between the variables. The standard error of the estimate shows the standard deviation of the residuals to be 0.00283724. This value can be used to construct prediction limits for new observations by selecting the Forecasts option from the text menu. The mean absolute error (MAE) of 0.00242825 is the average value of the residuals. The Durbin-Watson (DW) statistic tests the residuals to determine if there is any significant correlation based on the order in which they occur in your data file. Since the P-value is greater than 0.05, there is no indication of serial autocorrelation in the residuals at the 95.0% confidence level.

(2) Simple Regression - Activity concentration of ^{226}Ra vs. Activity concentration of ^{238}U

Activity Correlation Coefficient = 0.962777. The output shows the results of fitting a linear model to describe the relationship between Activity concentration of ^{226}Ra and Activity concentration of ^{238}U. The equation of the fitted model is :

$$C_{Ra} = 2.43438 + 5.28092* C_U \quad (12)$$

Where: CRa is Activity concentration of ^{226}Ra and CU is Activity concentration of ^{238}U. Since the P-value in the ANOVA table is less than 0.05, there is a statistically significant relationship between Activity concentration of ^{226}Ra and Activity concentration of ^{238}U at the 95.0% confidence level. The R-Squared statistic indicates that the model as fitted explains 92.694% of the variability in Activity concentration of ^{226}Ra. The correlation coefficient equals 0.962777, indicating a relatively strong relationship between the variables. The standard error of the estimate shows the standard deviation of the residuals to be 30.0613. This value can be used to construct prediction limits for new observations by selecting the Forecasts option from the text menu. The mean absolute error (MAE) of 22.4122 is the average value of the residuals. The Durbin-Watson (DW) statistic tests the residuals to determine if there is any significant correlation based on the order in which they occur in your data file. Since the P-value is less than 0.05, there is an indication of possible serial correlation at the

95.0% confidence level. Plot the residuals versus row order to see if there is any pattern that can be seen.

(3) Simple Regression Surface exhalation (Bq/kg day^{-1}) Activity concentration of ^{238}U

Activity Correlation Coefficient = 0.962777 and R-squared = 92.694 percent The output shows the results of fitting a linear model to describe the relationship between Surface exhalation (Bq/kg day^{-1}) and Activity concentration of ^{238}U. The equation of the fitted model is

Surface exhalation $*10^{-6} = 2.43438 + 5.28092* C_U$ (13)

Since the P-value in the ANOVA table is less than 0.05, there is a statistically significant relationship between Surface exhalation (Bq/kg day^{-1}) and Activity concentration of ^{238}U at the 95.0% confidence level. The R-Squared statistic indicates that the model as fitted explains 92.694% of the variability in Surface exhalation (Bq/kg day^{-1}). The correlation coefficient equals 0.962777, indicating a relatively strong relationship between the variables. The standard error of the estimate shows the standard deviation of the residuals to be 30.0613. This value can be used to construct prediction limits for new observations by selecting the Forecasts option from the text menu. The mean absolute error (MAE) of 22.4122 is the average value of the residuals. The Durbin-Watson (DW) statistic tests the residuals to determine if there is any significant correlation based on the order in which they occur in your data file. Since the P-value is less than 0.05, there is an indication of possible serial correlation at the 95.0% confidence level. Plot the residuals versus row order to see if there is any pattern that can be seen.

5- Elemental composition of phosphate

Phosphate rocks were mainly composed of CaO, P2O5, SiO2, Al2O3, SO3 and Fe2O3. The major components in phosphate rock were CaO, P2O5, SiO2, Al2O3, SO3, Fe2O3 and, to a lesser extent, Na2O, MgO, Cl, K2O, TiO2, V2O5 and MnO. In the samples, SiO2 may be found as quartz, and together with Al2O3 and Na2O and/or K2O. This result is similar to those published by. Who have studied phosphate soil rocks. Both of the major and minor components observed in this study were similar to those previously reported [24, 25–29].

6- The mineralogical composition of phosphate soil Analyzed by X-ray Diffraction

The 2θ angles of 31.86°, 32.18° and 33.02°, typical peaks of fluorapatite and hydroxyapatite $Ca_{10}(PO_4)_6(OH)_2$ were detected in sample (S1-S19) (Fig. 8a,b). The presence of hydroxyapatite, fluorapatite and carbonate hydroxyapatite was observed at the angles of 32.02°, 33.22° and 25.82° in sample (S1-S7) (Fig. 8.a,b). The presence of hydroxyapatite, and carbonate fluorapatite was observed at the angles of 26.62°, 29.38° and 29.44° in sample (S8-S19) (Fig. 8.a,b). Carbonate fluorapatite and hydroxyapatite were detected at the angles of 29.46° and 32.04° in sample (S12-S15) (Fig. 8.a,b). The peaks at 31.92° and 32.28° originated from hydroxyapatite were observed in sample (S13-S17) (Fig. 8.a,b). In addition to hydroxyapatite, the presence of fluorapatite and apatite was also observed at the angles of 33.08° and 25.92° in the XRD pattern of sample (S10, S11). Meanwhile, carbonate fluorapatite was also detected at the angle of 10.8° in sample S15 (Fig. 8.a,b). The angles of 31.84°, 29.48°, 25.86°, and 32.96° were detected in S13 and thus it was considered that sample (18-23) contained hydroxyapatite, carbonate fluorapatite, apatite and fluorapatite (Fig. 8.a,b). The results of X-ray powder diffraction analysis showed that the main minerals of the phosphate soil were apatite, fluorapatite and carbonate fluorapatite. These X-ray diffraction patterns of phosphate soil in this study were similar to those published by other authors who have studied phosphate rocks [32]. Phosphate soil samples of this study showed the presence of fluorapatite (Ca5F(PO4)3), apatite (Ca5(PO4)3(OH)), hydroxyapatite (Ca10(PO4)6(OH)2), carbonate hydroxyapatite Ca5(PO4, CO3)3(OH), carbonate fluorapatite (Ca5(PO4,CO3)3F), and quartz (SiO2). This composition was consistent with those published by other authors who have studied phosphate rocks from different places [31,32].

E. CONCLUSIN

The results of the present work indicate that the locations of natural investigation had normal level of natural background, except in location around Abou Zabal factory in sample from S0 to S6 and S20, S21 which showed relativity high concentration of ^{238}U, ^{40}K, ^{226}Ra and exhalation of ^{222}Rn, but still within the natural background level values sample from S7 to S19 and S22. These values are considered to be at a heights level for soil samples near the Abou Zabal factory area. The index of radioactivity in the sample near the factor its level was highest than unity which keeps the radiation hazard to be important. Determine levels of some natural radioactivity in soil samples were collected around Abou Zabal fertilizer phosphate factory in Egypt. Activity concentration of background radionuclides such as ^{226}Ra, ^{232}Th and ^{40}K of these samples was determined by using a high resolution γ ray co-axial HPGe gamma ray spectrometry and CR-39 detector. According to the results this analysis, ^{238}U was found concentration mean 241.06 Bqkg^{-1}, ^{226}Ra was found in concentrations mean of 283.87 Bq kg^{-1}; ^{232}Th in mean concentrations of 16.15, Bq kg^{-1}; and ^{40}K in mean concentrations of 146.36 Bq kg^{-1} for the analyzed soil, respectively.

Radon (^{222}Rn) mean concentration in the samples was estimated using solid state nuclear track detectors (CR – 39). The Radon gas mean doses from inhalation gas was found 337.06.37 µSv/y. Based on the radioactivity levels determined, the gamma-absorbed dose rates in soil sample above the ground were calculated. Elemental concentrations were determined for ^{226}Ra (range from 7.8 ppm to 46.26 ppm), ^{232}Th (range from 1.98 ppm to 9.14 ppm), ^{238}U (from 5.63 ppm to 33.28 ppm), and ^{40}K (from 0.07 % to 0.69 %). The measured Th/U ratio exhibits values was mean 0.17 , whereas the U/Ra ratio was mean 0.81 and Th/K ratio values was mean 0.8 there are unequilibrium between ^{232}Th and ^{40}K but there are equilibrium between ^{238}U and ^{226}Ra . Correlation Coefficient between Mass exhalation and Activity concentration of ^{238}U equal (1.0). Correlation Coefficient between Surface exhalation and Activity

concentration of ^{238}U equal (0.962777) this was very good correlation. Correlation Coefficient between Activity concentration of ^{226}Ra e and Activity concentration of ^{238}U equal (0.962777) this was very good correlation all are very good correlation. After analysing the XRD results we found the soil samples near the plant contain a high concentration of phosphate and its derivatives produced by the factory. And so we find that the high radioactivity in the soil samples vicinity of the plant concentration.

ACKNWLEGMENT

The authors wish to thank the staff of laboratory chemical warfare, radioactive materials department, the Egyptian Ministry of Defense for the helpful and cooperate contribution in achieving this work. The authors also thank workers the staff of Central lab. , National Center for Research and Technology NCRRT, Atomic Energy Authority, Cairo, Egypt.

III. HELPFUL

A. Figures and Tables

TABLE (1A) : The ratio between activity concentration and Elemental concentrations of ^{238}U, ^{226}Ra, ^{232}Th and ^{40}K

Sample	Th/U	Th/U(pm)	U/Ra	U/Ra(ppm)
S0	0.20	0.27	0.80	0.72
S1	0.16	0.22	0.79	0.71
S2	0.14	0.19	0.82	0.73
S3	0.16	0.22	0.82	0.73
S4	0.15	0.21	0.78	0.70
S5	0.13	0.19	0.78	0.70
S6	0.12	0.18	0.73	0.66
S7	0.13	0.19	0.77	0.69
S8	0.13	0.18	0.81	0.73
S9	0.09	0.12	0.80	0.72
S10	0.12	0.15	0.87	0.78
S11	0.11	0.12	1.07	0.96
S12	0.13	0.24	0.61	0.55
S13	0.18	0.46	0.42	0.38
S14	0.18	0.25	0.80	0.72
S15	0.17	0.23	0.80	0.72
S16	0.25	0.34	0.81	0.73
S17	0.16	0.23	0.75	0.67
S18	0.26	0.52	0.56	0.51
S19	0.24	0.38	0.71	0.64
S20	0.25	0.22	1.28	1.15
S21	0.24	0.22	1.24	1.12
S22	0.20	0.25	0.90	0.81
Mean	**0.17**	**0.24**	**0.81**	**0.73**
Max	**0.26**	**0.52**	**1.28**	**1.15**
Min	**0.09**	**0.12**	**0.42**	**0.38**

TABLE (1B) : The ratio between activity concentration and Elemental concentrations of ^{238}U, ^{226}Ra, ^{232}Th and ^{40}K

Sample	Raeq (Bq/Kg)	Th/Ra	Th/Ra(ppm)	Th/K	Th/K %
S0	568.37	0.07	0.20	1.95	124.55
S1	501.65	0.06	0.16	0.25	15.82
S2	438.39	0.05	0.14	0.14	9.25
S3	452.27	0.06	0.16	0.16	10.32
S4	459.09	0.05	0.15	0.15	9.77
S5	445.95	0.05	0.13	0.12	7.82
S6	431.30	0.04	0.12	0.10	6.62
S7	396.48	0.05	0.13	0.13	8.51
S8	362.05	0.05	0.13	0.10	6.36
S9	335.20	0.03	0.09	0.08	4.84
S10	323.27	0.04	0.12	0.09	5.73
S11	305.92	0.04	0.11	0.08	5.34
S12	337.94	0.05	0.13	0.10	6.35
S13	301.02	0.06	0.18	0.12	7.42
S14	257.09	0.06	0.18	0.10	6.35
S15	256.43	0.06	0.17	0.08	5.30
S16	264.46	0.09	0.25	0.13	7.99
S17	199.29	0.06	0.16	0.06	4.01
S18	153.71	0.10	0.26	0.07	4.19
S19	132.08	0.09	0.24	0.05	3.43
S20	111.29	0.09	0.25	0.05	3.18
S21	133.09	0.09	0.24	0.06	3.62
S22	152.85	0.07	0.20	0.05	3.43
Mean	**318.23**	**0.06**	**0.17**	**0.18**	**11.75**
Max	**568.37**	**0.10**	**0.26**	**1.95**	**124.55**
Min	**111.29**	**0.03**	**0.09**	**0.05**	**3.18**

TABLE (2A) : Activity concentration and Elemental concentrations of ^{238}U, ^{226}Ra, ^{232}Th and ^{40}K

Sample	A_U(Bq/Kg)	U (ppm)	A_{Ra}(Bq/Kg)	Ra (ppm)
S_0	462.60 ± 44.46	33.28	514.00 ± 48.06	46.26
S_1	410.85 ± 39.48	29.09	456.50 ± 42.68	41.09
S_2	359.10 ± 34.51	26.38	399.00 ± 37.31	35.91
S_3	325.70 ± 31.30	26.91	407.12 ± 38.07	36.64
S_4	332.20 ± 31.92	26.25	415.25 ± 38.83	37.37
S_5	324.10 ± 31.15	25.60	405.12 ± 37.88	36.46
S_6	316.00 ± 30.37	23.42	395.00 ± 36.93	35.55
S_7	289.10 ± 27.78	22.57	361.38 ± 33.79	32.52
S_8	278.59 ± 26.77	21.41	327.75 ± 30.64	29.50
S_9	264.30 ± 25.40	20.25	310.94 ± 29.07	27.98
S_{10}	250.01 ± 24.03	20.65	294.13 ± 27.50	26.47
S_{11}	254.99 ± 24.50	26.01	277.00 ± 25.90	27.00
S_{12}	321.14 ± 30.86	15.05	305.85 ± 28.60	27.53
S_{13}	185.80 ± 17.86	9.11	265.43 ± 24.82	23.89
S_{14}	112.50 ± 10.81	14.53	225.00 ± 21.04	20.25
S_{15}	179.42 ± 17.24	14.49	224.27 ± 20.97	20.18
S_{16}	178.83 ± 17.19	14.74	223.54 ± 20.90	20.12
S_{17}	181.93 ± 17.48	10.46	173.27 ± 16.20	15.59
S_{18}	129.15 ± 12.41	5.63	123.00 ± 11.50	11.07
S_{19}	69.45 ± 6.67	6.02	105.23 ± 9.84	9.47
S_{20}	74.35 ± 7.14	9.08	87.47 ± 8.18	7.87
S_{21}	112.07 ± 10.77	10.72	106.73 ± 9.98	9.61
S_{22}	132.30 ± 12.71	9.16	126.00 ± 11.78	11.34
Mean+ SD	**241.06** ± 23.17	**18.30**	**283.87** ± 26.53	**25.64**
Max	**462.60**	**33.28**	**514.00**	**46.26**
Min	**69.45**	**5.63**	**87.47**	**7.87**

Table (2B): Activity concentration and Elemental concentrations of ^{238}U, ^{226}Ra, ^{232}Th and ^{40}K

Sample	A_{th} (Bq/Kg)	T h (ppm)	A_k (Bq/Kg)	K %
S_{Row}	37.00 ± 0.19	9.14	19.00 ± 1.17	0.07
S_1	25.93 ± 0.13	6.40	104.80 ± 1.04	0.40
S_2	20.07 ± 0.10	4.96	138.80 ± 0.91	0.54
S_3	23.67 ± 0.12	5.85	146.70 ± 0.93	0.57
S_4	22.67 ± 0.12	5.60	148.44 ± 0.94	0.57
S_5	19.82 ± 0.10	4.90	162.10 ± 0.92	0.63
S_6	16.70 ± 0.09	4.12	161.30 ± 0.90	0.62
S_7	17.48 ± 0.09	4.32	131.31 ± 0.82	0.51
S_8	15.56 ± 0.08	3.84	156.50 ± 0.74	0.60
S_9	9.91 ± 0.05	2.45	130.90 ± 0.71	0.51
S_{10}	12.73 ± 0.06	3.14	142.00 ± 0.67	0.55
S_{11}	12.30 ± 0.06	3.04	147.20 ± 0.63	0.57
S_{12}	14.55 ± 0.07	3.59	146.60 ± 0.69	0.57
S_{13}	17.00 ± 0.09	4.20	146.60 ± 0.60	0.57
S_{14}	14.55 ± 0.07	3.59	146.59 ± 0.51	0.57
S_{15}	13.63 ± 0.07	3.37	164.50 ± 0.51	0.64
S_{16}	20.00 ± 0.10	4.94	160.00 ± 0.51	0.62
S_{17}	9.79 ± 0.05	2.42	156.10 ± 0.39	0.60
S_{18}	11.79 ± 0.06	2.91	179.88 ± 0.28	0.69
S_{19}	9.37 ± 0.05	2.31	174.70 ± 0.24	0.67
S_{20}	8.00 ± 0.04	1.98	160.80 ± 0.20	0.62
S_{21}	9.45 ± 0.05	2.33	166.80 ± 0.24	0.64
S_{22}	9.37 ± 0.05	2.31	19.00 ± 1.17	0.67
Mean	**16.15** ± 1.45	**3.99**	**146.36** ± **6.9**	**0.57**
Max	**37.00**	**9.14**	**179.88**	**0.69**
Min	**8.00**	**1.98**	**19.00**	**0.07**

Table (3): Radon doses inhalation, mass exhalation and surface exhalation

Sample	Effective radium concentration (Bq/kg)	Doses from inhalation gas (μsv/y)	Mass exhalation $*10^{-8}$ (bq/kg day^{-1})	Surface exhalation $*10^{-6}$ (bq/kg day^{-1})
S_0	10.46	608.16	122.94	81.82
S_1	9.29	540.13	109.19	72.67
S_2	8.12	472.1	95.43	63.51
S_3	8.28	481.71	97.38	64.81
S_4	8.45	491.32	99.32	66.10
S_5	8.24	479.34	96.90	64.49
S_6	8.04	467.36	94.48	62.88
S_7	7.35	427.58	86.44	57.53
S_8	6.67	387.79	78.39	52.17
S_9	6.33	367.9	74.37	49.50
S_{10}	5.98	348.01	70.35	46.82
S_{11}	5.64	354.95	66.25	44.09
S_{12}	6.22	361.88	73.15	48.69
S_{13}	5.40	314.05	63.49	42.25
S_{14}	4.58	266.22	53.82	35.82
S_{15}	4.56	265.36	53.64	35.70
S_{16}	4.55	264.49	53.47	35.58
S_{17}	3.53	205.01	41.44	27.58
S_{18}	2.50	145.53	29.42	19.58
S_{19}	2.14	124.51	25.17	16.75
S_{20}	1.78	103.49	20.92	13.92
S_{21}	2.17	126.29	25.53	16.99
S_{22}	2.56	149.08	30.14	20.06
Mean	**5.78**	**337.06**	**67.90**	**45.19**
Max	**10.46**	**608.16**	**122.94**	**81.82**
Min	**1.78**	**103.49**	**20.92**	**13.92**

Table (4): Radionuclide activity concentrations in sedimentary phosphate rock of different origin

Origin	Activity (Bq/kg)		
	^{238}U	^{232}Th	^{226}Ra
Present study	**241.06** ± 23.17	**16.15** ± 1.45	**283.87** ± 26.53
Florida	1500	16	1600
S. Carolina	4800	78	4800
Morocco	1700	30	1700
China	150	25	50
Egyot	523	16	218

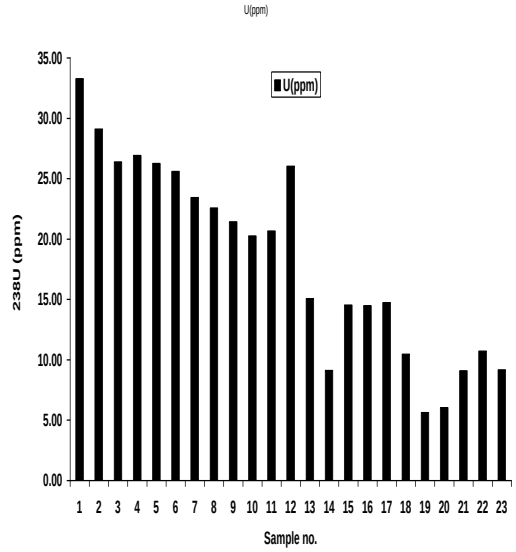

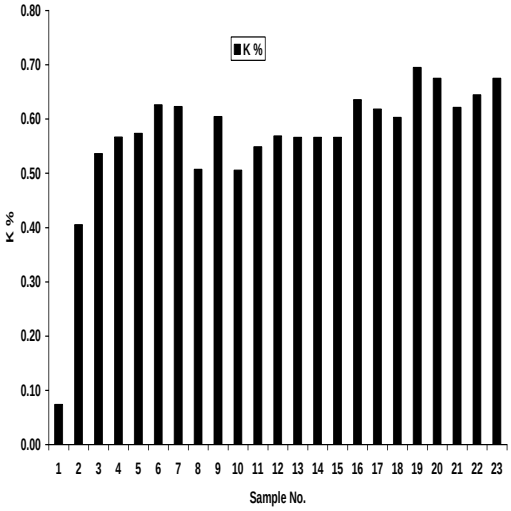

Fig (4.a.b.c.d) : Elemental concentrations of ^{238}U, ^{226}Ra, ^{232}Th (ppm) and ^{40}K (%) with soil sample

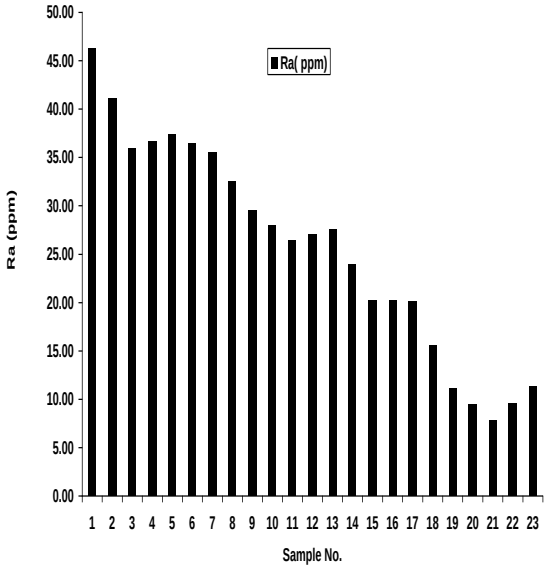

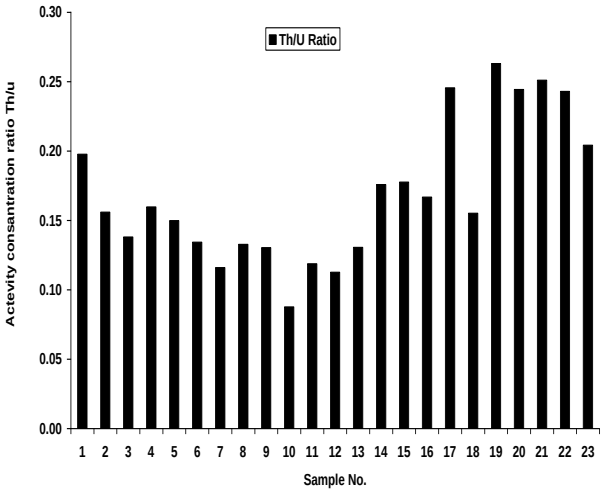

Fig (5) : $^{232}Th\backslash^{238}U$ ratio with soil sample

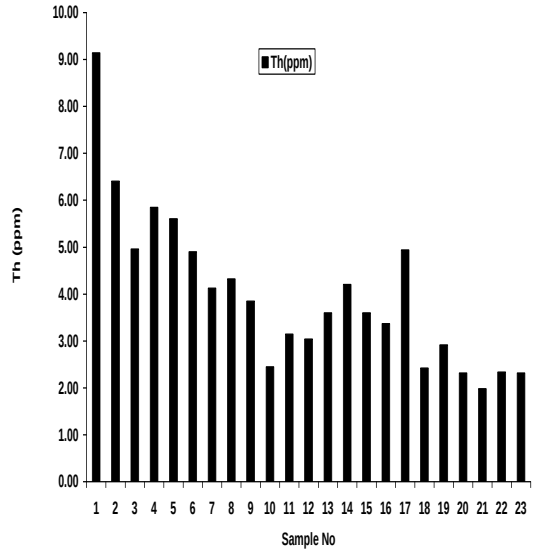

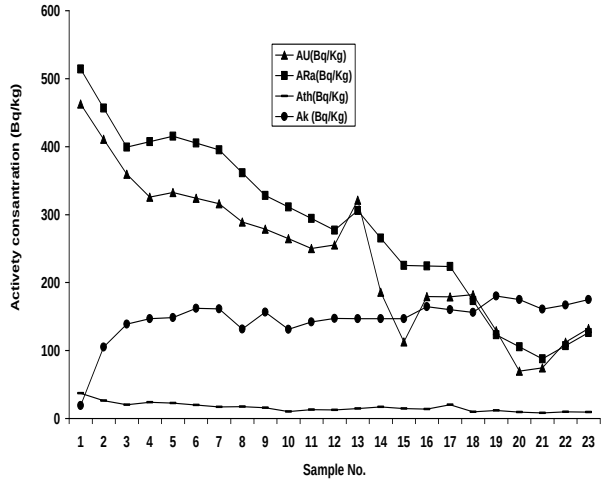

Fig (6): The activity concentration of ^{238}U, ^{232}Th, ^{226}Ra and ^{40}K

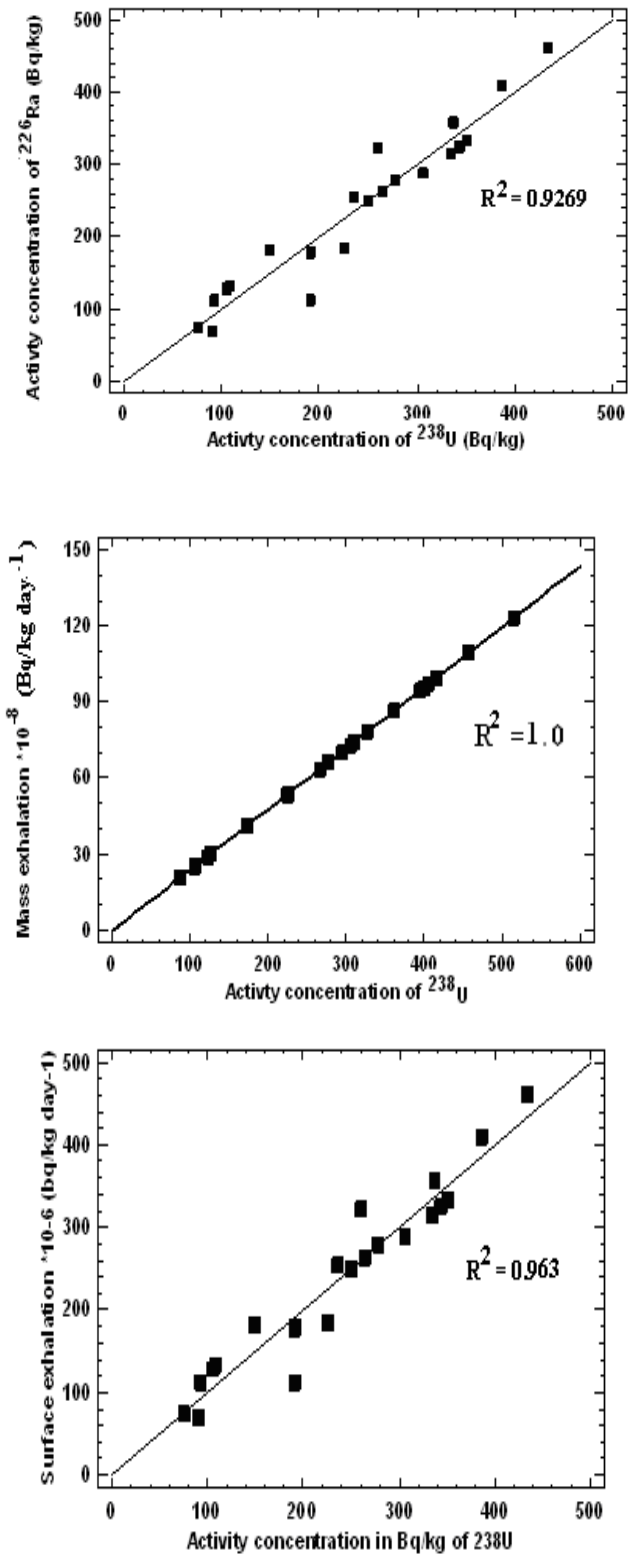

Fig (7): a Correlation between ^{226}Ra and ^{238}U in selected samples. b Correlation between mass exhalation of ^{222}Ra and ^{238}U in selected samples. c. Correlation between surface exhalation rate of radon and ^{238}U in selected samples

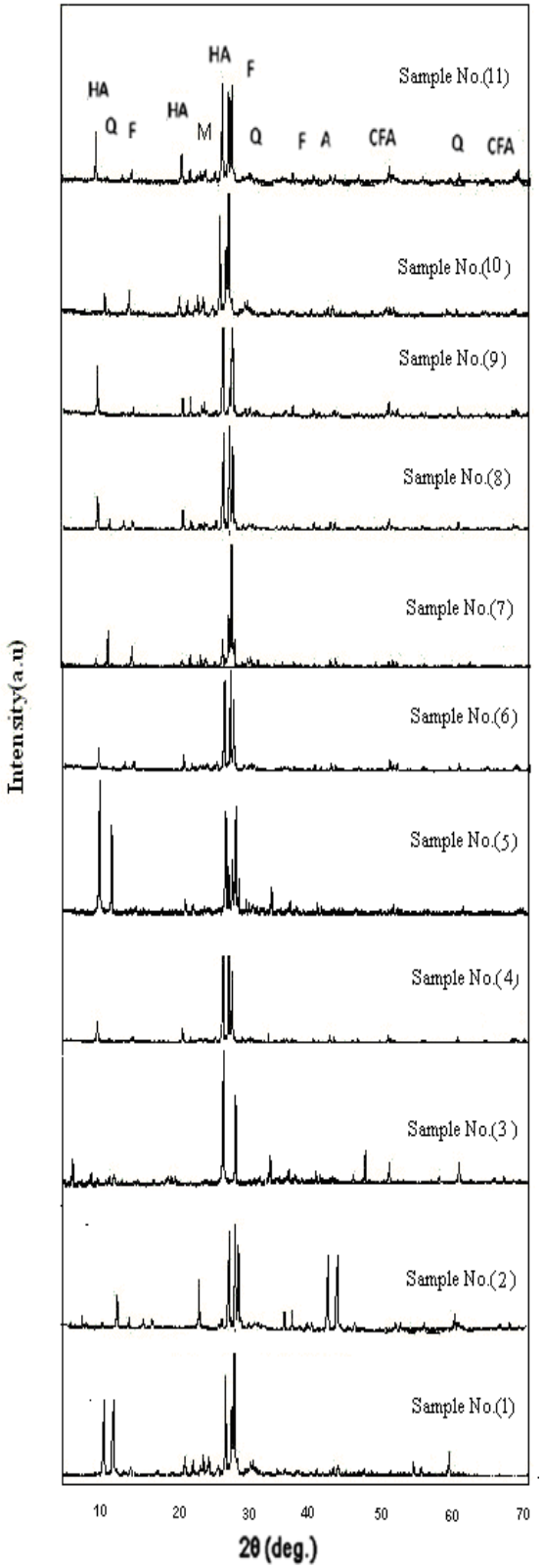

Fig. (8.A): X-ray diffraction diagram of phosphate soil from different sits. A=Apatite, CFA= Carbonate Fluor apatite, CH = Carbonate hydroxyapatite. F=Fluorapatite, HA=Hydroxyapatite, Q = Quartz

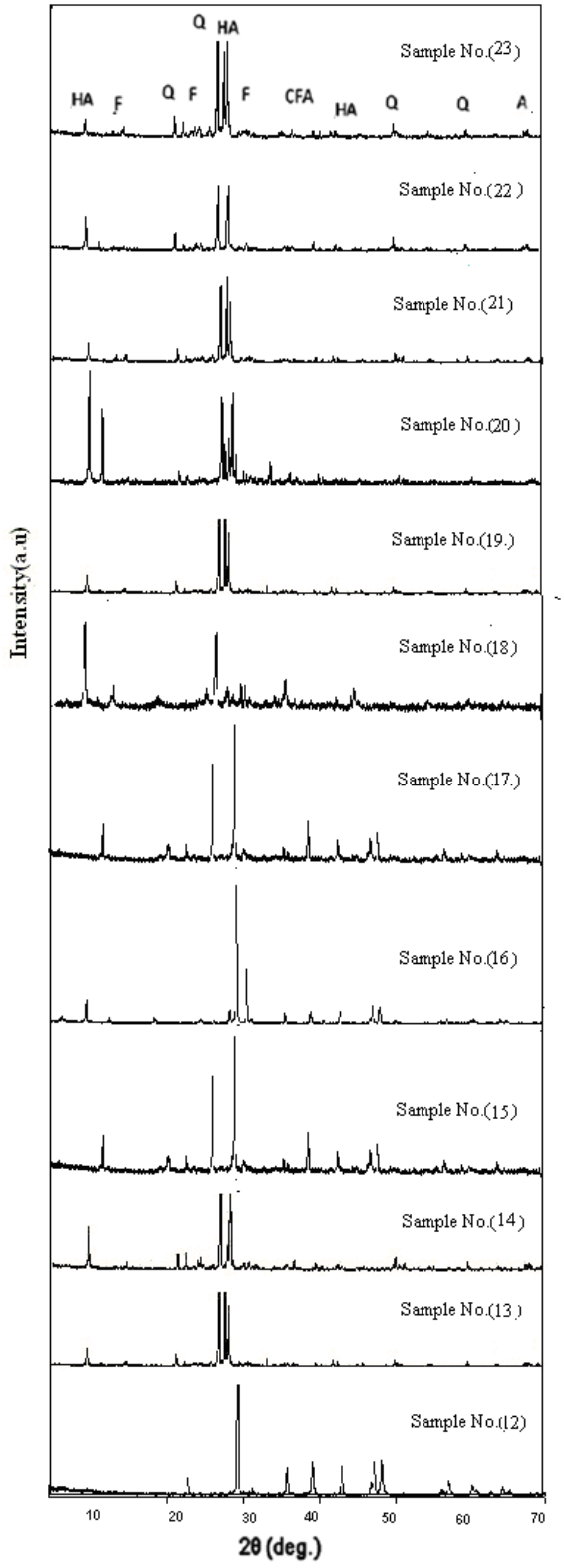

Fig. (8.B): X-ray diffraction diagram of phosphate soil from different sits. A=Apatite, CFA= Carbonate Fluor apatite, CH = Carbonate hydroxyapatite. F=Fluorapatite, HA=Hydroxyapatite, Q = Quartz

REFERENCES

[1] Mortvedt JJ, Sikora FJ , 1992. Heavy metal, radionuclides, and fluorides in phosphorus fertilizers. In F.J. Sikora, ed. Future directions for agricultural phosphorus research, pp. 69-73. TVA Bulletin Y-224. Muscle Shoals, USA.
[2] Brigden K, Stringer R, Santillo D , 2002. Heavy metal and radionuclide contamination of fertilizer products and phosphogypsum waste produced by the Lebanese Chemical Company. Greenpeace Research LAbouratories Technical Note 13/2002, November 2002: 16p. LCC_2002.pdf, 01.05.2006
[3] Smith, J. P. and Lehr, J. R. 1966. An X-ray investigation of carbonate apatites. Journal of Agricultural and Food Chemistry 14: 342-349.
[4] McClellan, G. H. and Lehr, J. R. 1969. Crystal chemical investigation of natural apatites. American Mineralogist 54: 1374-1391.
[5] Khater AE, Higgy R, Pimpl M (2001). Radiological impacts of natural radioactivity in Abu-Tartor phosphate deposits, Egypt. J. Environ. Radioact. 55(3):255-267.
[7] W. Chen, AndrewC. Chang,Wu. Laoosheng, Assessing long termenvironmental risks of trace elements in phosphate fertilizer, Ecotoxicol. Environ. Saf. 67 (2007) 48–58.
[8] Z.S. Altschuler, The geochemistry of trace elements in marine phosphorites. Part I. Characteristic abundances and enrichment, in: Y.K. Bentor (Ed.), Marine phosphorites, SEPM Spec. Publ., 1980
[9] C.A.Papachristodoulou, P.A. Assimakopoulos, N.E. Patronis, , K.G.Loannides, 2003. Use of HPGe gray spectrometry to assess the isotopic composition of uranium in soils. Journal of Environmental Radioactivity 64 (2–3), 195–203.
[10] R. M. Keyser, 1995, Characterization and Applicability of Low-Background Germanium Detectors, Technical Note, EG&G ORTEC, Oak Ridge, TN, USA.
[11] P.Hayumbu, M.B.Zaman, N.C.H.Lubaba, S.S. Munsanje, and D.Nuleya, J. Radioanal. Nucl. Chem.199, pp. 229-238,1995 .
[12] N.Lavi, F.Groppi, Z.B.Alfassi, 2004. On the measurement of ^{40}K in natural and synthetic materials by the method of high-resolution gamma ray spectrometry. Radiat. Meas. 38, 139e143.
[13] United Nations Scientific Committee on the Effects of Atomic Radiation (UNSCEAR). Sources and effects of ionizing radiation. Report of UNSCEAR to the General Assembly (2000).
[14] Azam A, Naqvi AH, Srivastava DS (1995) J Nucl Geophys 9:653–657
[15] UNSCEAR (1988) Sources effects and risks of ionizing radiation. Annex A, B, New York
[16] Abbady AGE (2004) J Appl Radiat Isotope 60:111–114
[17] Shetty PK, Narayana Y (2010) J Environ Radioactivity 101:1043–1047
[18] Marija J, Dragana T, Milovan S (2008) Radiat Meas 43:1448–1452
[19] Solecki AT (2002) J Geofiscia Int 41:339–344
[20] Ruixlang L (1986) Atom Energy Sci Technol 50:596–601
[21] Abbady AGE (2010) Appl. Radiat Isotopes 68:2020–2024
[22] Rajesh K, Sengupta D, Rajendra P (2003) Radiat Meas 36:551–553
[23] Mahur AK, Kumar Rajesh, Sonkawade RG, Sengupta D, Prasad Rajendra (2008) Nucl Instrum Method 266:1591–1597
[24] P.M. Rutherford, M.J. Dudas, R.A. Samek, Environmental impacts of phosphogypsum, Sci. Total. Environ. 149 (1994) 1–38.
[25] J.M. Arocena, P.M. Rutherford, M.J. Dudas, Heterogeneous distribution of trace elements and fluorine in phosphogypsum by-product, Sci. Total. Environ. 162 (1995) 149–160.
[26] J.E. Martín, R. García-Tenorio, M.A. Respaldiza, M.A. Ontalba, J.P. Bolívar, M.F. da Silva, TTPIXE analysis of phosphate rocks and phosphogypsum, Appl. Radiat. Isot. 50 (1999) 445–449.
[27] P.M. Rutherford, M.J. Dudas, J.M. Arocena, Radioactivity and elemental composition of phosphogypsum produced from three phosphate rock sources, Waste Manage. Res. 13 (1995) 407–423.
[28] F.T. Conceica, D.M. Bonotto, Radionuclides, heavy metals and fluorine incidence at Tapira phosphate rocks, Brazil, and their industrial byproducts, Environ. Pollut. 139 (2006) 232–243.
[29] E.M. ElAfifi,M.A. Hilal,M.F. Attallah, S.A. EL-Reefy, Characterization of phosphogypsum wastes associated with phosphoric acid and fertilizers production, J. Environ. Radioact. 100 (2009) 407–412.
[30] K. Komnitsa, A. Kontopoulos, I. Lazar, M. Cambridge, Risk assessment and proposed remedial actions in coastal tailings disposal sites in Romania, Miner. Eng. 11 (12) (1998) 1179–1190.
[31] P.M. Rutherford,M.J. Dudas, R.A. Samek, Environmental impacts of phosphogypsum, Sci. Total. Environ. 149 (1994) 1–38.
[32] K. Gnandi, H.J. Tobschall, Distribution patterns of rare-earth elements and uranium in tertiary sedimentary phosphorites of Hahotoé–Kpogamé, Togo, J. Afr. Earth Sci. 37 (2003) 1–10.